THERMAL AND STRUCTURAL RESPONSE OF THERMAL BREAK STRATEGIES IN STEEL BUILDING SYSTEMS

Kara D. Peterman[1], Julieta Moradei[1], James D'Aloisio[2], Mark Webster[3], Jerome F. Hajjar[1]

[1]Northeastern University
360 Huntington Avenue
Boston, MA

[2]Klepper Hahn and Hyatt
East Syracuse, NY

[3]Simpson Gumpertz and Heger
41 Seyon Street
Waltham, MA

ABSTRACT

In hot-rolled steel building systems, steel elements that pass through the building envelope—such as in cantilevered balconies and cladding systems—act as thermal bridges, transferring heat to and from the building exterior. This results in increased energy usage, which in turn increases environmental impact. To mitigate the effects of these thermal bridges, two approaches to thermal break strategies are proposed herein. The first approach examines the use of thermally improved materials (for example, fiber reinforced polymers and stainless steel) as shims and structural members while the second involves geometric thermal breaks such as intermittently spaced members and slotted members. The proposed strategies are thermally validated via parametric studies using the Heat3 software packages. From the thermal analysis results, the configurations resulting in the greatest reduction in thermal transmittance will be structurally validated with both computer models and experimental testing. The goal of this ongoing research is to introduce new mitigation strategies for reducing thermal transmittance in building structures for adoption into engineering practice and implementation into the design codes.

1. INTRODUCTION

This study of thermal break strategies for cladding systems in steel structures aims to propose effective structural thermal breaks and validate them through extensive modeling and experimental testing. Thermal bridge mitigation strategies examined in this work range from inserting a thermally-improved shim into the bolted structural connections to replacing the structural member entirely with a thermally-improved member. Two materials explored to date include the use of fiber reinforced polymers (FRPs) and stainless steel. As FRPs differ in mechanical properties to steel, it is necessary to validate the behavior for these FRP fills in common thermal bridges, typically found in cladding details installed on steel structures.

Three cladding details are explored in this research: the slab-supported shelf angle, roof posts for supporting mechanical units, and cantilevered canopy beams. Shelf angles represent a continuous

thermal bridge as the shelf angle bears on the interior structural system around the perimeter of the building, and at every story. Roof posts and canopy beams represent point thermal bridges, which span the building envelope only at discrete locations.

A typical detail for slab-supported shelf angles is shown in Figure 1, with an example of a thermally-improved shim installed at the connection locations. Adding shims to the connection locations is a two-fold benefit: while the thermally-improved material is now bridging the building envelope instead of steel, the shelf angle is also offset from the slab by the shims, and the air layer created by this offset provides additional insulation. Shelf angle shims are limited in size to the recommendations in AISC Design Guide 22: Façade Attachments to Steel-Framed Buildings (Parker, 2008), in this case, the height of the shelf angle vertical leg, and 3 inches in width.

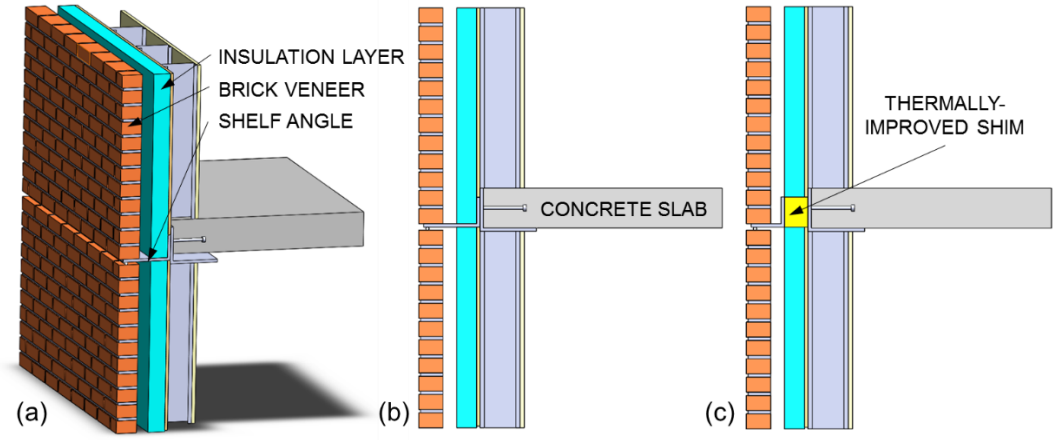

Figure 1: Typical slab-supported shelf angle details (a) isometric view (b) elevation view of unmitigated detail (c) elevation view of mitigated detail, with a (3x4 inch, 3 inch thick) thermally-improved shim installed at the connection location.

Figure 2 illustrates the roof post detail, demonstrating shim mitigation with a thermally-improved shim installed beneath the end plate (welded to the post itself). Unlike the shelf angle shims, the size of shims for point thermal break strategies is bounded only by the connecting geometry—in this case, the width of the interior beam and the size of the roof post end plate.

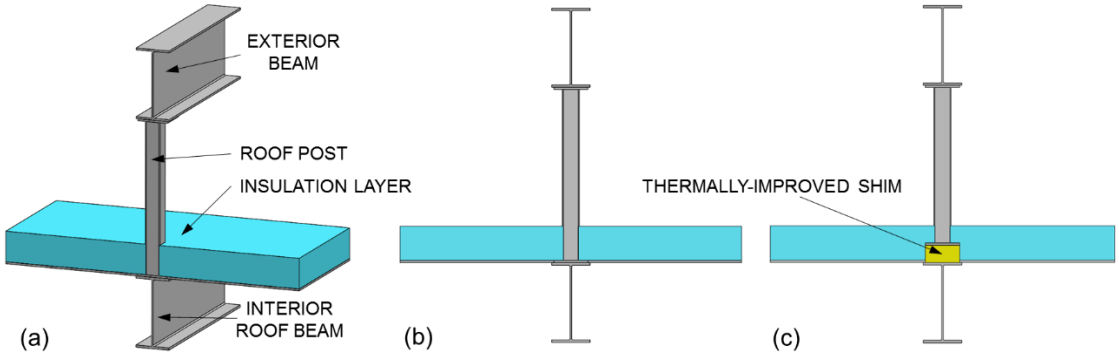

Figure 2: Typical roof post detail (a) isometric view (b) elevation view of unmitigated detail (c) elevation view of mitigated detail with a thermally-improved shim installed beneath the post end plate (equal in area and geometry to the end plate).

Canopy beams are mitigated similarly to roof posts—via a shim at the base of the end plate, identical in size (or larger) than the end plate. The most significant difference between canopy beam and roof post is that canopy beams extend horizontally from the walls, through the veneer of the structure, while roof posts are vertical members on the roof. This difference in function manifests itself in different section sizes and design loads, discussed in Section 3 of this work.

Thermally-improved materials explored in this research include vinyl ester FRP, polyurethane FRP, phenolic FRP, and two proprietary products, known here as "Proprietary 1" and "Proprietary 2." Thermal modeling on the three subsystems is presented, as well as existing structural test results and an overview of future structural testing. While the scope of the project as a whole includes creep testing at the material-level for the thermally-improved shims, and double-lap splice bolted steel connection testing, these efforts are not detailed herein.

2. THERMAL MODELING RESULTS

Thermal modeling was conducted in HEAT3 v7 (Blomberg 2001), for the thermal break strategies proposed for the cladding details explored in this work. Modeling was conducted in three-dimensions to validate these proposed strategies for details as they would be installed and constructed in a typical building. Results for the three cladding details are summarized below.

While the configurations modeled in HEAT3 are analogous to those considered for structural testing, there are a few key differences. In the structural testing, specimens are over-designed to ensure failure is forced away from the connections, in order to observe structural behavior further from the design spectrum. HEAT3 requires that curved surfaces are approximated as straight lines segments and that the surfaces of adjacent materials must be in contact (required for the transmission of thermal energy). Air layers are modeled with distinct coefficients of thermal-conductivity (analogous to an insulation layer) to avoid non-contact surfaces in the model. While bolt holes would typically be slightly larger than the bolt shaft diameters, they are in direct contact for modeling purposes only.

Interior and exterior boundary conditions are prescribed in Normative Appendix A of ASHRAE 90.1-2013 and NFRC 100-2014. R-values for air films are specified in Para. A9.4.1 of ASHRAE 90.1-2013 (for these models, exterior air film is R-0.17 hr-ft^2-°F/Btu and interior air film is R-0.68 hr-ft^2-°F/Btu). As interior and exterior boundary condition temperatures are not specified, they are based on the NFRC values provided in Para. 4.3.2.D of NFRC 100-2014. An interior ambient temperature of 69.8°F and an exterior ambient temperature of –0.4°F were assumed, in accordance with NFRC-2014.

2.1 Thermal modeling: slab-supported shelf angles

Two-dimensional renderings of the three-dimensional thermal gradient results for the slab-supported shelf angle detail are shown in Figure 3. Note that with the addition of a thermally-improved shim, the shelf angle is shorted such that the air cavity in the wall remains constant regardless of mitigation.

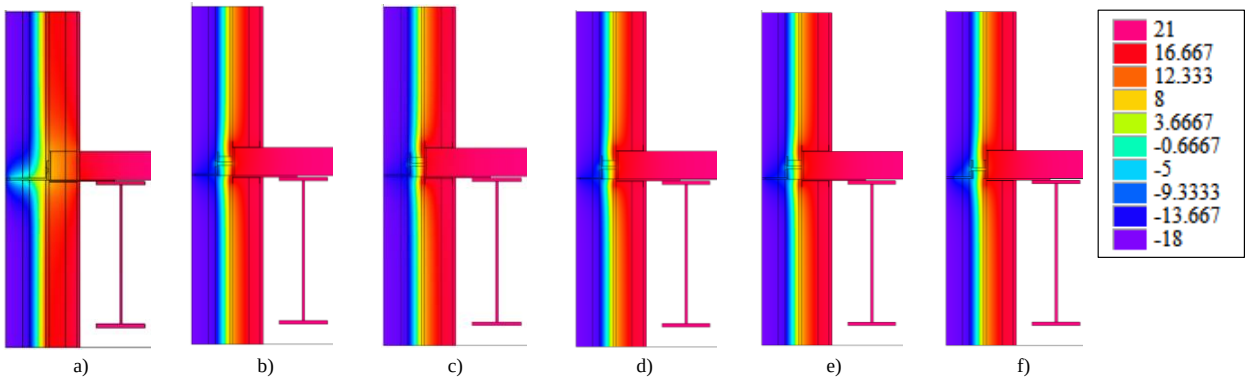

Figure 3: Thermal gradients of a) Unmitigated, b) Vinylester shim with A325 bolts (ΔU-value=50.22%), c) Vinylester shim with A304-SH bolts (ΔU-value=53.16%), d) Proprietary 1 shim (ΔU-value=54.32%), e) Proprietary 2 shim (ΔU-value=54.05%), f) Stainless tube shim (ΔU-value=47.73%) – units in degrees Celcius. (Peterman et al, 2016).

As shown in Figure 3, bolt material (stainless steel vs carbon steel) and shim material are varied to produce improvements in thermal conductivity (U-value) ranging from 47% to 54%. This improvement in U-value is from several sources: the thermally-improved shims; the shortened shelf angle size, resulting in less steel in the detail; the use of stainless steel bolts; and intermittent spacing between connection points. Results are detailed and tabulated in Table 1 below.

Table 1: Thermal modeling results from shelf angle modeling efforts (Peterman et al, 2016)

Unmitiagated Model			Mitigated Model				Comparison	
Model Name (-)	Bolt Type (-)	U-Value (BTU/h*ft2*°F)	Model Name (-)	Shim Material (-)	Bolt Type (-)	U-Value (BTU/h*ft2*°F)	Δ U-Value (BTU/h*ft2*°F)	%-Reduction
Shelf Angle Unmitigated 2.5 Inch_S1_V2	A304-SH	0.138	Shelf Angle Mitigated 2.5 Inch_S8_V3	Vinylester shim	A325	0.082	0.056	40.41
Shelf Angle Unmitigated 2.5 Inch_S1_V2	A304-SH	0.138	Shelf Angle FRP 2.5 Inch_S19	FRP angle	A304-SH	0.072	0.066	47.94
Shelf Angle Unmitigated 5 Inch_S4_V2	A304-SH	0.112	Shelf Angle Mitigated 5 Inch_S14.1_V3	Vinylester shim	A325	0.056	0.056	50.22
Shelf Angle Unmitigated 5 Inch_S4_V2	A304-SH	0.112	Shelf Angle Mitigated 5 Inch_S14.2_V3	Vinylester shim	A304-SH	0.053	0.060	53.16
Shelf Angle Unmitigated 5 Inch_S4_V2	A304-SH	0.112	Shelf Angle Mitigated 5 Inch_S17_V3	Proprietary 1 shim	A304-SH	0.051	0.061	54.32
Shelf Angle Unmitigated 5 Inch_S4_V2	A304-SH	0.112	Shelf Angle Mitigated 5 Inch_S18.1_V3	Proprietary 2 shim	A304-SH	0.052	0.061	54.05
Shelf Angle Unmitigated 5 Inch_S4_V2	A304-SH	0.112	Shelf Angle Mitigated 5 Inch_S18.2_V3	Stainless tube shim	A304-SH	0.059	0.054	47.73

2.2 Thermal modeling: roof posts

Two-dimensional views of the roof post thermal modeling results are shown in Figure 4 below. Insulation contributes significantly to the overall thermal performance of the sub-system, so the insulation thickness is varied in addition to shim material and thickness.

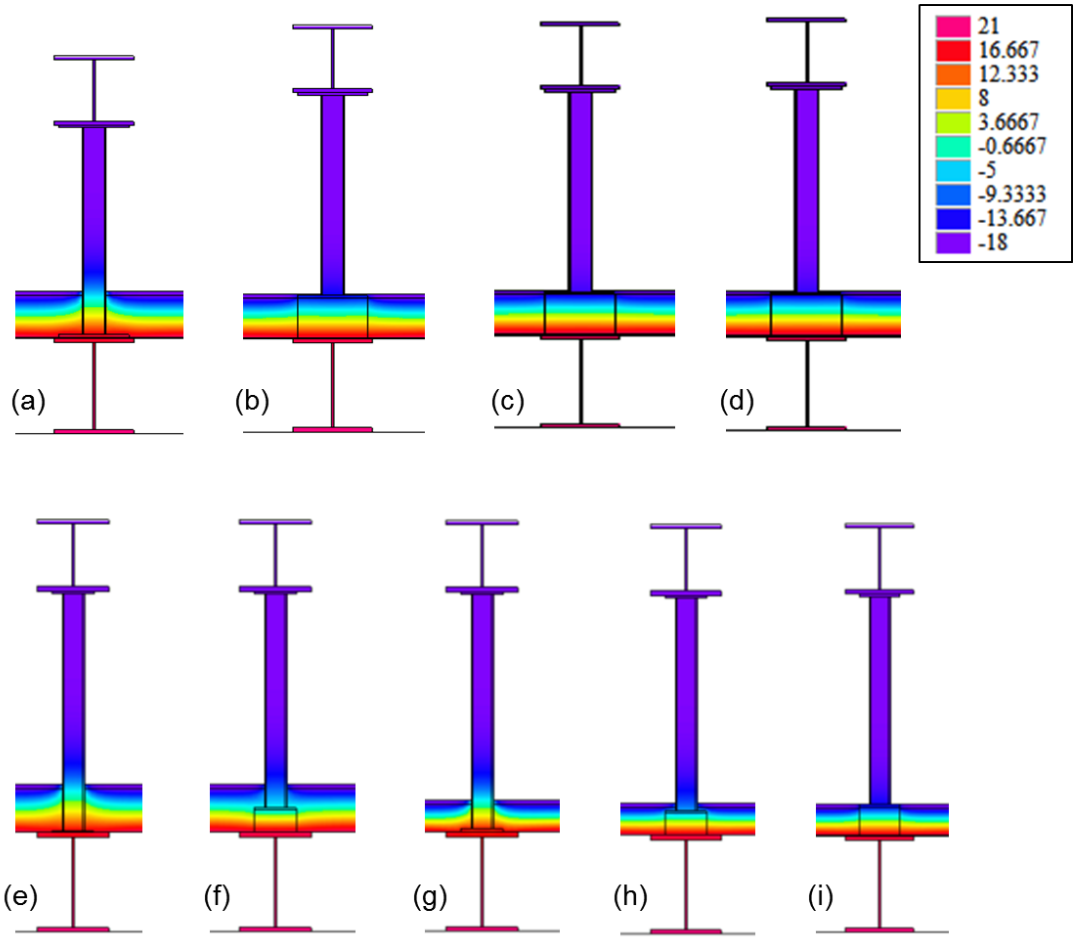

Figure 4: Thermal modeling roof posts 2D results and comparisons: a) Unmitigated (R1), b) Vinylester shim (U-value 5.15% reduction), c) Proprietary 1 shim (U-value 13.5% reduction), d) Proprietary 2 shim (U-value 11.75% reduction) e) Unmitigated 6 inch insulation (0.0363 U-value), f) Mitigated 6 inch insulation and 3 inch vinylester shim (U-value 9.64% reduction), g) Unmitigated 3.8 inch insulation (0.0535 U-value), h) Mitigated 3.8 inch insulation and 3 inch vinylester shim (U-value 9.72% reduction), i) Mitigated 3.8 inch insulation and 4 inch vinylester shim (U-value 9.91% reduction)

Improvement in U-value ranges from 9% to 13.5%, and is dependent on the thermal conductivity of the thermally-improved shim, and insulation layer. Because the roof post thermal bridge only exists at discrete points along a rooftop, improvements in thermal conductivity appear small when compared to those observed in the shelf angle results. Future studies on uninterrupted roof surfaces

(a best case scenario for this detail) will be conducted to better frame these results. Complete results are shown in Table 2.

Table 2: Selected thermal modeling results from roof post modeling efforts

Unmitiagated Model		Mitigated Model			Comparison	
Model Name (-)	U-Value (BTU/h*ft2*°F)	Model Name (-)	Shim Material (-)	U-Value (BTU/h*ft2*°F)	Δ U-Value (BTU/h*ft2*°F)	%-Reduction
R1 - UNMITIGATED ROOF POST - ZONE 7	0.0349	R2 - MITIGATED 6 IN VINLESTER ROOF SHIM - ZONE 7	Vinylester shim	0.0331	0.0018	5.16
R1 - UNMITIGATED ROOF POST - ZONE 7	0.0349	R11 - MITIGATED 6 IN PROPRIETARY 1 ROOF SHIM - ZONE 7	Proprietary 1 shim	0.0302	0.0047	13.47
R1 - UNMITIGATED ROOF POST - ZONE 7	0.0349	R12 - MITIGATED 6 IN PROPRIETARY 2 ROOF SHIM - ZONE 7	Proprietary 2 shim	0.0308	0.0041	11.75
Mitigated model with shim material removed	0.0535	R2 - MITIGATED 3 IN VINYLESTER ROOF SHIM - 3,8 IN INSULATION - ZONE 7	Vinylester shim	0.0483	0.0052	9.72
Mitigated model with shim material removed	0.0363	R2 - MITIGATED 3 IN VINYLESTER ROOF SHIM - 6 IN INSULATION - ZONE 7	Vinylester shim	0.0328	0.0035	9.64
Mitigated model with shim material removed	0.0535	R2 - MITIGATED 4 IN VINYLESTER ROOF SHIM - 3,8 IN INSULATION - ZONE 7	Vinylester shim	0.0482	0.0053	9.91

2.3 Thermal modeling: canopy beams

Canopy beam thermal modeling results are presented in Figure 5 below. This cladding detail, in which the beam protrudes horizontally from the wall veneer, behaves similarly to the roof posts, with the exception that insulation layer is strictly defined in ASHRAE 90.1, and is not varied as a part of the thermal modeling survey.

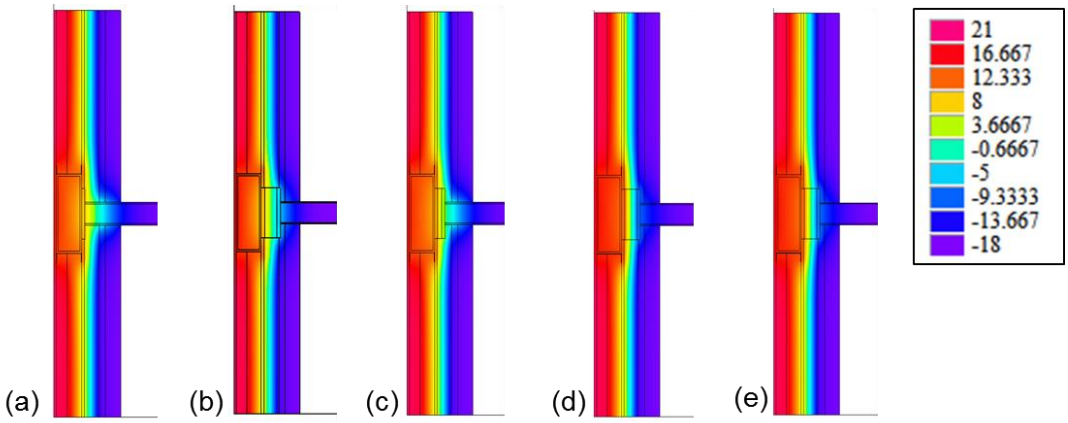

Figure 5: Thermal modeling of canopy beams 2D results and comparisons: a) Unmitigated (CB1), b) Vinylester shim with 3" thickness (U-value 4.11% reduction), c) Vinylester shim with 1" thickness (U-value 1.32% reduction), d) Proprietary 1 shim (U-value 13.07% reduction), e) Proprietary 2 shim (U-value 11.45% reduction)

Thermal conductivity of the thermally-improved shim, in addition to shim thickness dictate the variation in improved in U-value, with improvement ranging between 1% for thinner shims and 13% for thicker shims. These results are further detailed in Table 3 below. As with the roof posts,

improvements in thermal conductivity are limited by the discrete nature of the point cladding detail. Work on uninterrupted wall details remains to be completed to bound these results.

Table 3: Selected thermal modeling results from canopy beam modeling efforts

Unmitiagated Model		Mitigated Model				Comparison	
Model Name (-)	U-Value (BTU/h*ft2*°F)	Model Name (-)	Shim Material (-)	Shim Thickness (in)	U-Value (BTU/h*ft2*°F)	Δ U-Value (BTU/h*ft2*°F)	%-Reduction
CB1	0.0681	CB2	vinylester shim	3	0.0653	0.00	4.11
CB1	0.0681	CB3	proprietary 1 shim	3	0.0592	0.01	13.07
CB1	0.0681	CB4	proprietary 2 shim	3	0.0603	0.01	11.45
CB1	0.0681	CB9	vinylester shim	1	0.0672	0.00	1.32

3. STRUCTURAL TESTING OF SUB-SYSTEMS

Structural testing of successful mitigation strategies is currently in progress at Northeastern University. Cladding details are tested at full scale, to failure, to simulate the range of possible behaviors in as-built structures. At the time of this paper, shelf angle testing is complete and results are presented herein. Roof posts and canopy beams are underway, and the test matrices and test rigs are discussed in this work.

3.1 Shelf angle structural testing

To simulate the as-built sub-system in the laboratory environment, shelf angles were bolted to a rigid steel slab, acting as a rigid concrete floor slab. Specimens were tested with efficiently designed connections (5/8" dia. bolts) and over-designed connections (bolts with diameter ¾" or 1"). In compliance with the Climate Zones outlined in ASHRAE 90.1, shelf angles designed for thinner wall cavities (Climate Zone 1: 1.5" shims and L6x4x5/16 angles) and thicker wall cavities (Climate Zone 7: 3" shims and L7x4x3/8 angles) were considered. Shim materials were varied, and additional mitigation strategies were also explored: all-FRP angle (S19), shims constructed of HSS3x3x3/8 (S20), and shims made of carbon steel (S21, to explore the structural impact of intermittent spacing). These variables are detailed in Table 4.

Table 4: Shelf angle test matrix, from Peterman et al, 2016

		Mitigation Strategy			Specimen Information			
Test Name	**Specimen Type**	**Type**	**Material**	**Thick (in)**	**Length**	**Section**	**Bolt/Stud Spec**	**Bolt Dia. (in)***
S1	designed	-	-	-	42	L6x4x5/16	A325	0.625
S2	designed	-	-	-	42	L6x4x5/16	A304-SH	0.75
S3	over-designed	-	-	-	42	L6x4x5/16	A325	1
S4	designed	-	-	-	42	L7x4x3/8	A325	0.625
S5	designed	-	-	-	42	L7x4x3/8	A304-SH	0.75
S6	over-designed	-	-	-	42	L7x4x3/8	A325	1
S7	over-designed	shim	vinylester	1.5	42	L6x4x5/16	A325	1
S8	designed	shim	vinylester	1.5	42	L6x4x5/16	A325	0.625
S9	over-designed	shim	polyurethane	1.5	42	L6x4x5/16	A325	1
S10	over-designed	shim	phenolic	1.5	42	L6x4x5/16	A325	1
S11	over-designed	shim	proprietary 1	1.5	42	L6x4x5/16	A325	1
S12	over-designed	shim	proprietary 2	1.5	42	L6x4x5/16	A325	1
S13	over-designed	shim	vinylester	3	42	L7x4x3/8	A325	1
S14	designed	shim	vinylester	3	42	L7x4x3/8	A325	0.625
S15	over-designed	shim	polyurethane	3	42	L7x4x3/8	A325	1
S16	over-designed	shim	phenolic	3	42	L7x4x3/8	A325	1
S17	over-designed	shim	proprietary 1	3	42	L7x4x3/8	A325	1
S18	over-designed	shim	proprietary 2	3	42	L7x4x3/8	A325	1
S19	over-designed	FRP angle	vinylester	-	42	FRP L6x4x1/2	A325	1
S20	over-designed	tube shim	carbon steel	HSS3x3x3/8	42	L7x4x3/8	A325	1
S21	over-designed	steel shim	carbon steel	3	42	L7x4x3/8	A325	1

*holes are standard holes (bolt diamter + 1/16 inch)

The angles were tested in a large steel reaction frame located at Northeastern University. The load beam acts to simulate loads on the shelf angle from brick veneers, and moves along sliders such that the load remains in the vertical plane. This is illustrated in Figure 6.

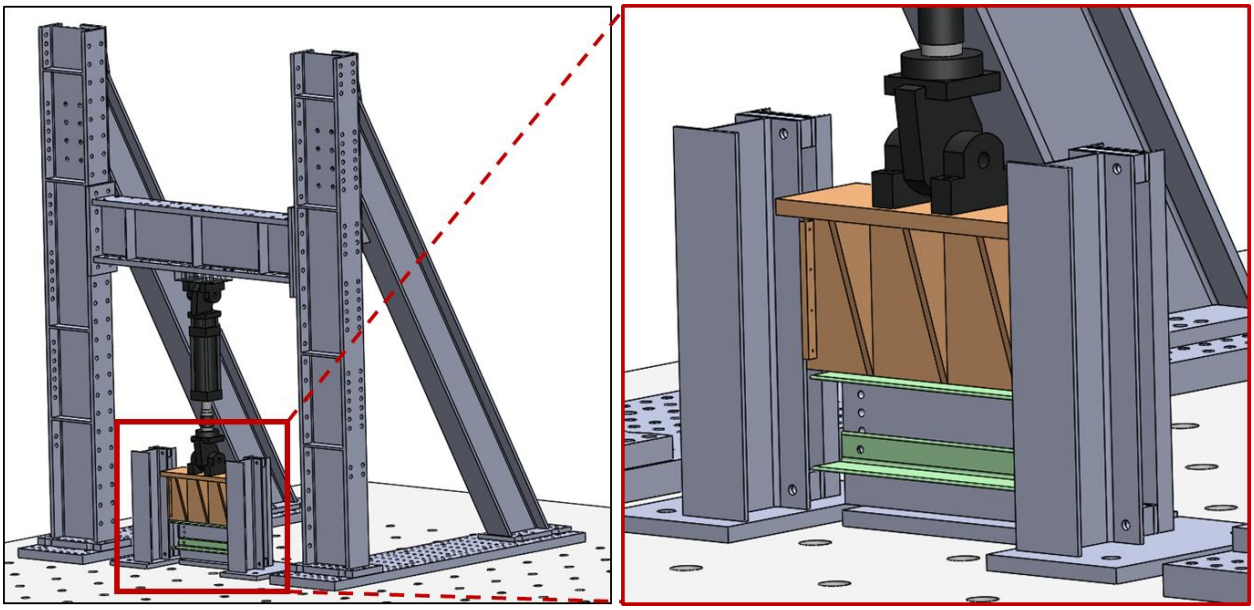

Figure 6: Schematic of test rig demonstrating load beam configuration and specimen installation (Peterman et al, 2016).

Vertical force vs. vertical displacement results are shown in Figures 7 (Climate Zone 7 specimens) and 8 (Climate Zone 1 specimens), measured at the actuator, with the typical design region shown in the inset plot.

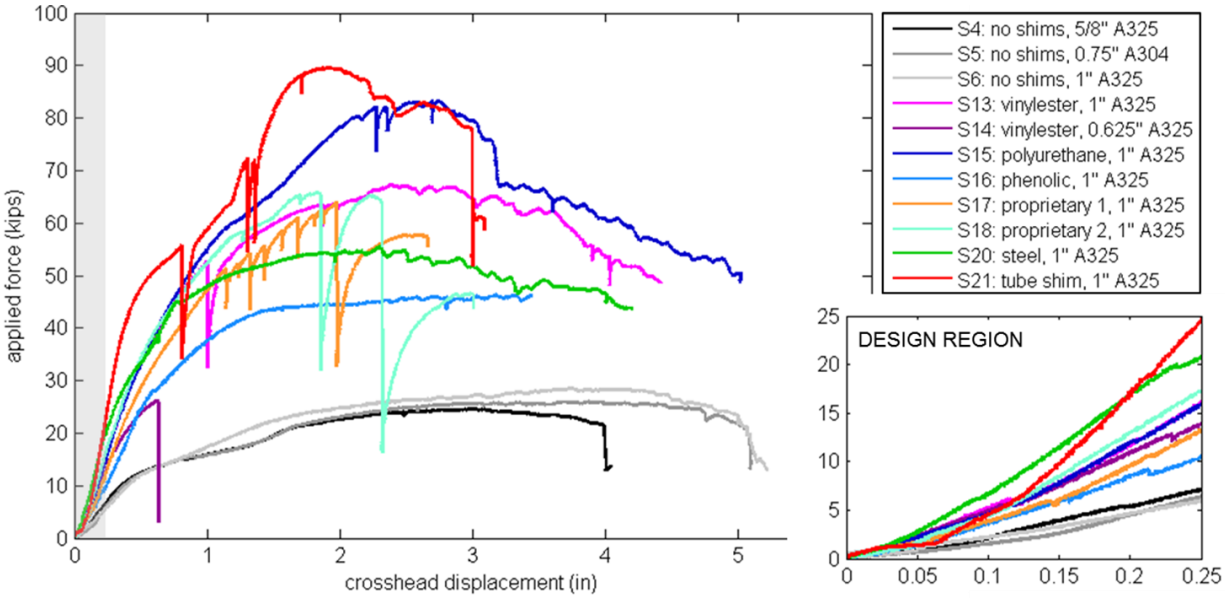

Figure 7: Climate Zone 7 (5 inch wall cavity, corresponding to 3 inch shims and L7x4x3/8 angles) shelf angle force vs. displacement results, with the design region (displacement of 0.25 inch at vertical leg) shown in inset (adapted from Peterman et al, 2016).

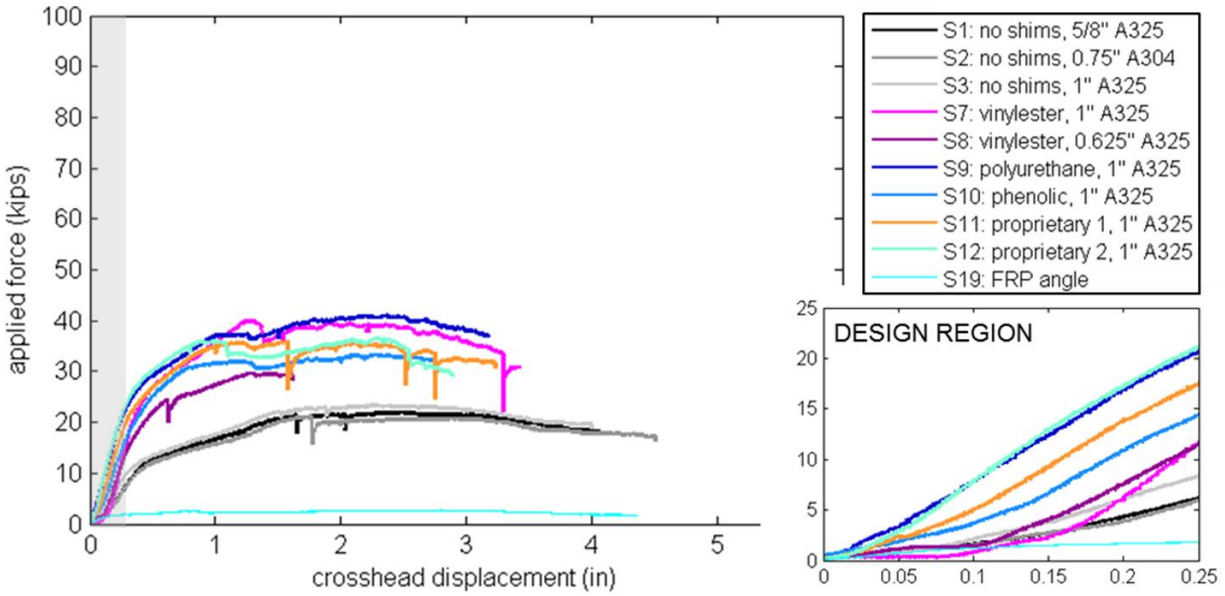

Figure 8: Climate Zone 7 (2.5 inch wall cavity, corresponding to 1.5 inch shims and L6x4x1/2 angles) shelf angle force vs. displacement results, with the design region (displacement of 0.25 inch at vertical leg) shown in inset.

Mitigation strategies do not result in a decrease in strength or stiffness from the original unmitigated details. It is important to note that because the wall cavity thickness must remain constant between mitigated and unmitigated details, the shelf angles benefit from reduced moment on the horizontal angle leg, as the leg is loaded closer to the vertical leg with a shim than without a shim. Thus, while shimmed specimens appear to experience significant strength gains from the unmitigated detail, this is anticipated, and should not be considered as related to the shims themselves. For the Climate Zone 7 specimens, the results are bracketed by the unmitigated system and the 3 inch steel shim specimen—illustrating the difference in behavior between the geometries, assuming shims are rigid. However, the stiffness of the mitigated details in the design region exceeds those of the unmitigated detail, suggesting that shim mitigation could serve as a structurally-feasible thermal break.

Observed failure modes are demonstrated in Figure 9. In specimens with strong shims (S21, S20, S15, S9), the shelf angle fractured at the heel. While shims did crush and delaminate, this failure mode was only observed well beyond the design region, at 1+ inches of displacement. For the Climate Zone 1 results (Figure 8), the thinner shelf angle controls much of the behavior. While angle deformation was consistent in all of the tests, the thinner angles failed prior to the shims. For these specimens, the shims did not crush, but simply delaminated, or did not fail.

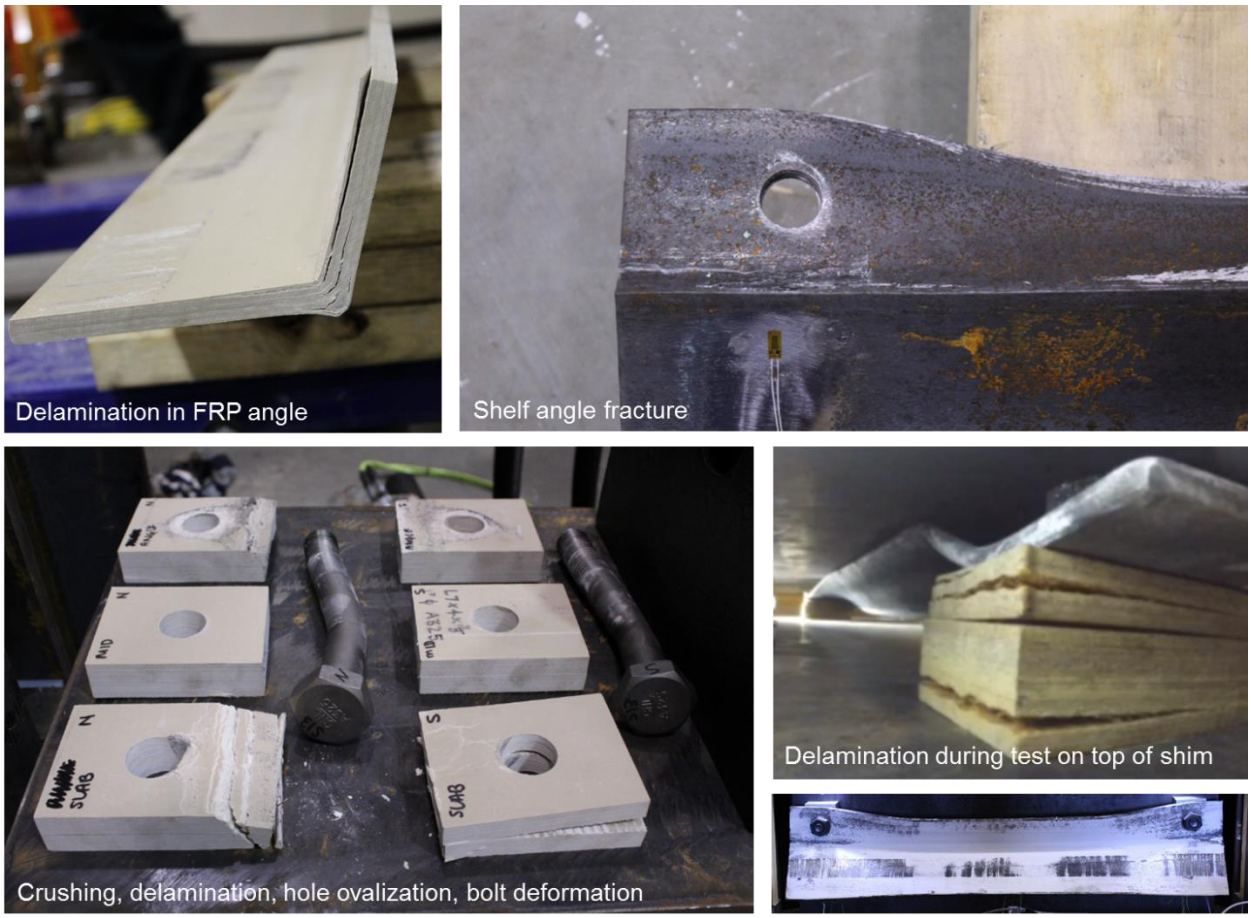

Figure 9: Failure modes in shelf angle testing, including shim crushing, shim delamination, angle fracture, and deformation of the shelf angle (bottom right).

3.2 Roof post and canopy beam structural testing

Utilizing the same test frame as in the shelf angle testing (shown in Figure 10) roof posts and canopy beam tests are currently underway. Also analogous to the shelf angles, efficiently designed specimens and over-designed specimens are considered. In the over-designed details, end plates are up-sized, as are rod diameters. Additionally, welds between the post and beam and the end plates are CJP welds. This is unique to this test program, to ensure that the welds do not fracture prematurely. Rods are also tested in high strength stainless steel (B8 Class 2) and standard A36 carbon steel (A307). Shims vary in thickness between 1 and 3 inches. FRP sleeves are also considered in the test program, consisting of a FRP HSS section surrounding the standard steel post, connected via through-thickness threaded rods. Not shown in the test matrices (Table 5) are the top plate details. Across all post and beam specimens, they are over-designed as 1 inch thick to direct forces into the bottom of the specimen.

Roof posts are designed as 30 inch HSS3x3x3/16 while canopy beams are designed as 66 inch HSS4x4x1/2, to accommodate larger design forces. Since roof posts support mechanical units, they are loaded with axial and lateral loads, while canopy beams are loaded with lateral forces alone, as in a pure cantilever.

Table 5: Roof post and canopy beam test matrices

ROOF POSTS (axial + lateral)

		MITIGATION STRATEGY			SPECIMEN INFORMATION				
Test Name	Specimen Type	Type	Material	Thick (in)	End Plate	Rod Dia. (in)	Rod Spacing (in)	Rod Spec	Loading
R1	designed	-	-	-	9x9x3/8"	0.5	6" oc	B8 Class 2	Monotonic
R2	designed	shim	vinylester	3	9x9x3/8"	0.5	6" oc	B8 Class 2	Monotonic
R3	designed	sleeve	FRP 4x4x1/2	-	9x9x3/8"	0.5	6" oc	B8 Class 2	Monotonic
R4	designed	-	-	-	9x9x3/8"	0.5	6" oc	B8 Class 2	Cyclic
R5	designed	shim	vinylester	3	9x9x3/8"	0.5	6" oc	B8 Class 2	Cyclic
R6	designed	sleeve	FRP 4x4x1/2	-	9x9x3/8"	0.5	6" oc	B8 Class 2	Cyclic
R7	over-designed	-	-	-	9x9x1/2"	0.75	6" oc	A307	Cyclic
R8	over-designed	shim	vinylester	3	9x9x1/2"	0.75	6" oc	A307	Cyclic
R9	over-designed	shim	phenolic	3	9x9x1/2"	0.75	6" oc	A307	Cyclic
R10	over-designed	shim	polyurethane	3	9x9x1/2"	0.75	6" oc	A307	Cyclic
R11	over-designed	shim	proprietary 1	3	9x9x1/2"	0.75	6" oc	A307	Cyclic
R12	over-designed	shim	proprietary 2	3	9x9x1/2"	0.75	6" oc	A307	Cyclic
R13	over-designed	shim	vinylester	1	9x9x1/2"	0.75	6" oc	A307	Cyclic
R14	over-designed	sleeve	FRP 4x4x1/2	-	9x9x1/2"	0.75	6" oc	A307	Cyclic

CANOPY BEAMS (lateral)

		MITIGATION STRATEGY			SPECIMEN INFORMATION				
Test Name	Specimen Type	Type	Material	Thick (in)	End Plate	Rod Dia. (in)	Rod Spacing (in)	Rod Spec	Loading
C1	designed	-	-	-	9x9x3/8"	0.75	6" oc	B8 Class 2	Monotonic
C2	designed	shim	vinylester	3	9x9x3/8"	0.75	6" oc	B8 Class 2	Monotonic
C4	designed	-	-	-	9x9x3/8"	0.75	6" oc	B8 Class 2	Cyclic
C5	designed	shim	vinylester	3	9x9x3/8"	0.75	6" oc	B8 Class 2	Cyclic
C7	over-designed	-	-	-	9x9x1/2"	1	6" oc	A307	Cyclic
C8	over-designed	shim	vinylester	3	9x9x1/2"	1	6" oc	A307	Cyclic
C9	over-designed	shim	phenolic	3	9x9x1/2"	1	6" oc	A307	Cyclic
C10	over-designed	shim	polyurethane	3	9x9x1/2"	1	6" oc	A307	Cyclic
C11	over-designed	shim	proprietary 1	3	9x9x1/2"	1	6" oc	A307	Cyclic
C12	over-designed	shim	proprietary 2	3	9x9x1/2"	1	6" oc	A307	Cyclic
C13	over-designed	shim	vinylester	1	9x9x1/2"	1	6" oc	A307	Cyclic
C15*	over-designed	-	-	-	9x9x1/2"	1	6" oc	A307	Cyclic

**Test C15 is to be tested at (30 inches) rather than 66 inches, as in the remainder of the canopy beam tests*

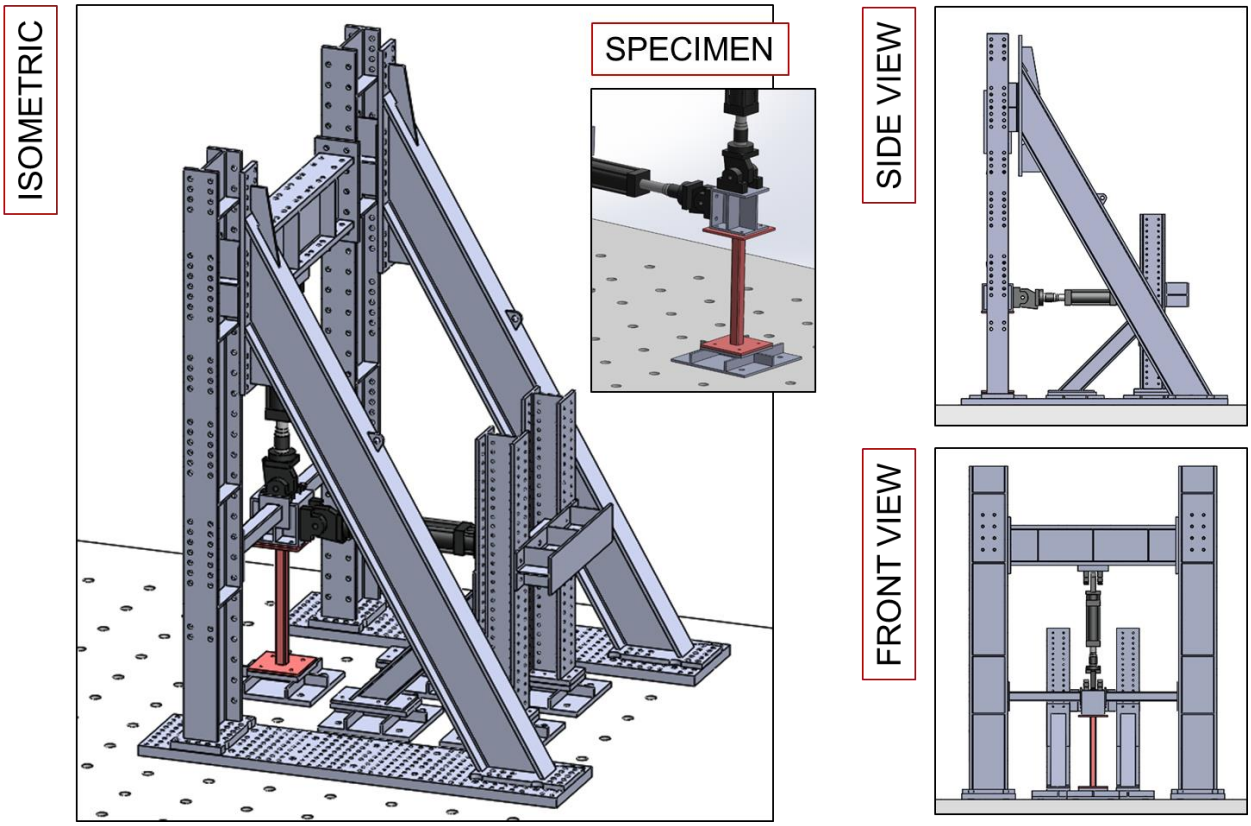

Figure 10: View of roof post and canopy beam test rig, demonstrating multi-degree of freedom loading (vertical and horizontal actuators, applying axial and lateral loads, respectively) and specimen installation.

For the roof posts, axial load is applied to the specimen and held in displacement control while the lateral actual pushes either monotonically or cyclically to failure. In the canopy beam tests, the vertical actuator is removed.

4. CONCLUSIONS AND FUTURE WORK

This paper summarizes recent research on strategies for breaking the thermal bridge in connections in steel building cladding details, including shelf angles, roof posts, and canopy beams. Extensive thermal modeling is detailed herein, demonstrating the effectiveness of thermal break strategies for cladding systems in steel buildings. While the thermal conductivity of shelf angle details are significantly improved by the addition of thermally-improved shims, the roof posts and canopy beams have more modest improvements due in part to their non-continuous use in typical structures. Shelf angle structural testing demonstrates promise: mitigated sub-systems do not experience a decrease in strength or stiffness from the unmitigated details. Work is in progress to further analyze the data collected from this series of tests. Roof posts, canopy beams, creep testing, and connection testing all are underway in ongoing research to fully characterize the structural performance of these thermal break strategies.

5. ACKNOWLEDGEMENTS

This material is based upon work supported by the Charles Pankow Foundation, the American Institute of Steel Construction, the American Composites Manufacturers Association (ACMA), the ACMA-Pultrusion Industry Council, Schöck AG, the National Science Foundation under Grant No. CMMI-0654176, Simpson Gumpertz & Heger Inc., Klepper Hahn and Hyatt, and Northeastern University. Any opinions, findings, and conclusions expressed in this material are those of the authors and do not necessarily reflect the views of the sponsors. The authors would like to acknowledge Kyle Coleman, Michael McNeil, Kurt Braun, Justin Kordas, Madeline Augustine, and Dennis Rogers of Northeastern University, project team members Pedro Sifre, Mehdi Zarghamee, James Parker, Sean O'Brien, Jason Der Ananian, and Jessica Coolbaugh (formerly) of Simpson Gumpertz & Heger and the members of the Industrial Advisory Panel and the ACMA Pultrusion Industry Council Technical Advisory Team.

6. REFERENCES

1. American Institute of Steel Construction (AISC) (2005). Specification for Structural Steel Buildings, ANSI/AISC 360–05, AISC, Chicago, Illinois.
2. American Institute of Steel Construction (AISC) (2010). Specification for Structural Steel Buildings, ANSI/AISC 360–10, AISC, Chicago, Illinois.
3. ASHRAE 90.1 (2013). Energy Standard for Buildings Except Low-Rise Residential Buildings (I-P edition), ANSI/ASHRAE/IES Standard 90.1-2013.
4. Blomberg, T. (2001). "Heat3: A PC program for heat transfer in three dimensions: Manual with brief theory and examples." Lund-Gothenberg Group for Computational Building Physics.
5. Parker, James. (2008), American Institute of Steel Construction (AISC) Steel Design Guide 22: Façade Attachments to Steel-Framed Buildings. AISC, Chicago, Illinois.
6. Peterman, K.D., Moradei, J., D'Aloisio, J.A., Webster., M.D., Hajjar, J.F. (2016). "The behavior of double-lap splice bolted steel connections with fiber-reinforced polymer fills. Proceedings of the Connections VIII Workshop, Boston, MA.